THE USE OF PHYSICS ENGINES IN QUANTIFYING BREAKWATER DAMAGE

I M A GLEDHILL*, J M GREBEN, A K COOPER**, R DE VILLIERS** AND J-H GROBLER***

***Defence, Peace, Safety and Security Operational Unit**
****Built Environment Operational Unit**

CSIR, PO Box 395, Pretoria 0001
Tel: 011 841-2769, Email: IGLEDHIL@csir.co.za

ABSTRACT

The response of proposed breakwater packing strategies to incident waves is usually tested and evaluated in a model hall. There is currently also increasing interest in using numerical simulations to model both the packing of a breakwater, and its response to storms. In this paper, we test the use of physics engine software, which provides fast modelling of hundreds of units, as a means of gaining insight into damage quantification and breakwater disorder.

Both dolosse and Antifer armour units are investigated. An order parameter P_2 is proposed which is shown, using the numerical models, to be a useful measure of orientational order or disorder when the randomness of the packing is in question. A root-mean-square displacement parameter is proposed as a measure of the movement of armour units from their original positions under cyclic forces. Both parameters are easy to use in simulations, and the use of these parameters in model halls and in the field is discussed.

1 INTRODUCTION

Breakwaters protect coastal assets and infrastructure along the coastline of South Africa. They are designed for stability and resistance to wave damage and storms, and the design is based on experience and experiment; model halls are used to test designs, and predict their suitability for the application. In parallel with scaled experiments and measurements in the field, there is increasing interest in numerical simulation of breakwater dynamics. This involves three challenging areas: the purely structural interaction of hundreds of armour units, the adequate simulation of waves, and the coupling of the fluid and structure (Figure 1).

In this paper, we explore the use of parameters to answer two questions: “How much change has taken place in armour unit position?” and “How random is the packing?” The first question is related to damage and stability, and the use of a root-mean-square displacement measure δ_{rms} has been proposed for this purpose (Greben et al., 2012). The second question is prompted by the assessment of packing strategies, which can be traced, at last partially, to measures of orientational order. A suitable parameter P_2 has been adopted from the physics of liquid crystals (see below) as an orientational order parameter.

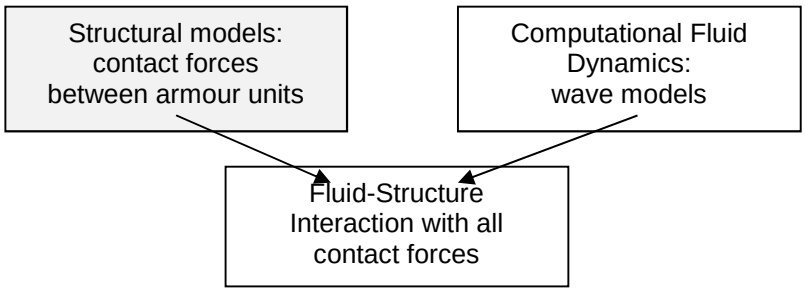

Figure 1. Pure structural models, pure fluid models, and fluid-structure interaction

Note that this paper is confined to the purely mechanical contact modelling problem of the structural aspects of breakwaters, considered as granular media. No detailed fluid modelling or fluid-structure interaction is considered in this work, since those aspects are being undertaken in other tasks in a multidisciplinary project. Work on plunging wave turbulence and free-surface modelling is a parallel task (Govender et al., 2002), (Mukaro et al., 2010), in which new methods are becoming available, as is coupling of fluids with moving structures using the full contact force model developed here (Grobler et al., 2010). It should also be noted that this work deals solely with packing and interlocking issues, and is not directed at material properties such as material strength, shrinkage, or concrete type. The concrete density choice is described below. Friction is covered by a simple stick-slip law for the purposes of shape interactions. Energy lost in collisions (by deformation, minor fracturing, *etc.*) is accounted for through an empirical coefficient of restitution, also described below.

With numerical modelling, detailed data on each individual armour unit becomes available, including translational and rotational displacement. This has prompted a considerable amount of work (for example (Latham et al., 2002), (Latham et al., 2008), (Xiang et al., 2010), (Dentale et al., 2009)) towards numerical schemes of use in coastal engineering. Rigid body dynamics may be modelled in several ways. The most widely used of these is the Discrete Element Method (DEM) (e.g. (Cundall & Strack, 1979), (Owen et al., 2004)). From these, the Combined Finite-Element/Discrete-Element Method has grown (Munjiza, 2004), (Munjiza, 2011), which is a promising new way of investigating the dynamics of granular media, including force chains and fracture failure. DEM schemes have been interfaced with Navier-Stokes codes (Latham et al., 2008), (Araki & Deguchi, 2011) with considerable success. An alternative modelling strategy for multiple rigid bodies has been adopted in the present work due to its advantages in speed. DEM models are detailed but time-consuming, particularly when mutual collisions between of the order of thousands of particles of irregular shape must be considered. We have therefore tested the use of a physics engine (Greben et al., 2012), as described below, and the physics engine PhysX has also been interfaced with free-surface Navier-Stokes fluid models (Grobler et al., 2010).

It should be noted that, as in other fields in which numerical simulation has reached mature development for some decades, computer modelling does not replace experiment

or field observation. In aeronautics, for example, test facilities offer wind tunnel capabilities integrated with Computational Fluid Dynamics and flight test, balancing the costs involved, the confidence levels attainable, and risk management for the design outcome. Where the effect of breakwater packing strategy on stability is important (van der Meer, 1995), (Frens et al., 2008), simulation can provide supplementary insight, and a test bed for trials.

When a breakwater is inspected in the field, it is possible to obtain positions of the units in the top layer by photogrammetry. Optical fiducial methods for measuring orientation are also under development (Vieira et al., 2008), which are quickly becoming more accurate as the technology develops. This opens a path for validation with field data.

The background theory and a description of the physics engine model are provided in section 2. The two parameters δ_{rms} and P_2 are defined and their origins summarised. Because a numerical breakwater is a numerical model, relying on a certain number of random variables for simulation purposes, the stochastic nature of the packing is investigated in section 3, by varying the random height field representing the irregular underlayer. In section 4, the effect of the height of variations in the underlayer is assessed for a model dolos packing. The dolos armour unit is chosen because of its irregular interlocking shape, and a packing is devised which allows the variation to be seen clearly. The possible interdependence of δ_{rms} and P_2 is checked. In contrast to dolos packing, Antifer units are usually packed in a highly regular fashion, and section 5 shows the application of δ_{rms} and P_2 in such a case. It is concluded that the two parameters have different applications. The displacement parameter δ_{rms} is suited to before-and-after scenarios, while P_2 has merit where a snapshot of orientation is available.

2 COMPUTATIONAL METHODS AND THEORY

2.1 Physics engine

Physics engine software was developed to take advantage of the rapid development of Graphical Processing Units (GPUs) prompted by the fast-growing market for animation, visualisation, robotics and virtual environments. The physics engine chosen for present purposes is PhysX™ (NVIDIA, 2012). The components of a physics engine are object representation, collision detection, collision processing, and particle kinematics. Each body is represented by a tetrahedral mesh model. It is important that PhysX™ provides the ability to manage collisions between polyhedral units, such as Antifers and dolosse, since in most DEM methods, particles are approximated by multiple spheres – which are unsuitable for this application, in which flat planes are in sliding contact. Rigid body collisions are based on the constraint models of Hahn (Hahn, 1988). Collision detection is based on a scheme of bounding boxes, and a contact graph keeps a record of interactions between moving bodies and immovable boundaries. In a collision, particle boundaries may overlap or “overshoot”. To manage overshoot, a skin width for maximum overlap is specified by the user, and the collision is integrated back in time until the overlap is less than the skin width, using the contact graph (Müller et al., 2008). Contact normals, normal velocities, and tangential velocities before and after the collision are calculated for each collision, together with the updated position and orientation for each particle, nd are subject to conservation equations and constraints. Static and dynamic friction and a coefficient of restitution for the objects are formulated within the constraints. Chatter is controlled by a “sleep” mode: velocities are unchanged when the kinetic energy in a collision falls below a threshold. This mode allows a collection of particles to rest in equilibrium, instead of constantly adjusting due to minor collisions.

In actual collisions between concrete units, some energy is dissipated through deformation and minor fracture. The energy lost in this process is approximated through the coefficient of restitution on the numerical model.

2.2 Armour units and packing

A right-handed coordinate system is defined as follows: *x* runs in the coastwise direction, *y* is vertical, and *z* is in the inland direction (Figure 2).

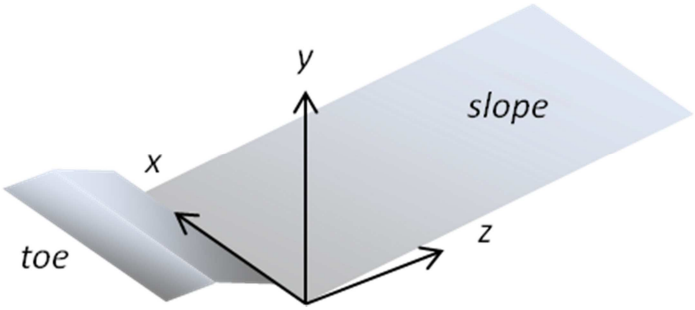

Figure 2. Static axis system

An impermeable fixed slope in the *z* direction forms the underlayer. A toe of 2 m top depth and 10 m base depth with height 1.8 m is placed in the –*z* region. The origin of the simulation is located at the intersection of the slope with the toe, midway along the simulation in the coastwise direction. Walls confine the boundaries at minimum and maximum *x.* The centre of gravity of the *i*-th unit is $\overline{c_i} = (x_i, y_i, z_i)$. Angular displacement is described by three Euler angles $(\phi_i, \theta_i, \psi_i)$, applied as rotations in the order of Tait-Bryan angles: the unit is rotated by $\phi_i$about the *x* axis, then by θ_i about the intermediate *y'* axis, and then about ψ_i about the final *z"* axis.

In order to model an irregular underlayer, the slope is composed of 1 m squares. The centre of each of these may be lowered by a random height to form an irregular heightfield. The maximum amplitude of these hollows is *h*.

The material properties of the units and the underlayer are those of concrete, of density 2350 kg/m^3, coefficient of restitution 0.05, static and dynamic friction both 0.75 (0.6 is the usual coefficient of the friction of concrete on rock, but surface preparation is important and we use the higher value to compensate for the lack of interlocking between armour units and the heightfield), and linear and angular damping both 0.9, to model air and water resistance (Greben et al., 2012). The geometries of 17 t dolosse were kindly provided by the CSIR Built Environment Coastal Engineering and Port Infrastructure group. Dolosse and Antifers are modelled at full scale, but can be simulated at the scale of model halls if required. The units are lowered with the shank parallel to the y axis at a constant velocity of 0.5 ms^{-1} until they are in contact with another object, after which they fall under gravity. An orientational axis for each dolos, $\widehat{Y_i}$, is defined as a normal to the shank. The angle between the *y* axis and $\widehat{Y_i}$ is defined as w_i. The dolos units are packed as described below, and the slope angle may be varied.

Antifer units, which are tapered cubes with side grooves, are laid in a more ordered fashion and initially form a more regular structure (Van der Meer & Heydra, 1991). The slope angle is chosen as 26.6º. The slope is 20 m high and has a horizontal crest. Walls provide boundaries in *x* and a toe is present.

It is useful to observe the action of a perturbing force on the units. For the purposes of providing an oscillating disturbance that approximates wave action, a simple model has been devised as follows. A force *F* is exerted on points on the upper and lower surfaces of units at points determined by ray casting normal to the slope (details are provided in an extended paper (Greben et al., 2012)).

$$F = F_0\left[i_z \cos(\omega t - kz) + i_y \sin(\omega t - kz)\right]\varphi(y), \qquad 0 \le t \le nT$$
$$\boldsymbol{F = 0}, \qquad \boldsymbol{t > nT} \quad (1)$$

$$\varphi(y) = H(y_{SWL} - y)H(y - y_{min})\frac{y - y_{min}}{y_{SWL} - y_{min}} + H(y - y_{SWL})H(y_{max} - y)\frac{y_{max} - y}{y_{max} - y_{SWL}},$$
$$\boldsymbol{H(y) = 0, y < 0;\ H(y) = 0.5, y = 0;\ H(y) = 1, y > 0} \quad (2)$$

Here F_0 is the force amplitude, i_y and i_z are unit vectors in y and z, $\omega=2\pi/T$, t, and k are frequency, time and wave number respectively, n and T are the number of waves and the period respectively, φ is a function that is maximum at the still water line (subscript *SWL*), and zero for y outside a minimum (subscript *min*) and maximum (subscript *max*) height. The minimum, still water, and maximum levels are y_{min} = 5.658 m, y_{SWL} = 15.568 m, and y_{max} =23.568 m respectively. Better wave approximations are of course easy to formulate, but, as it is noted above, more realistic models are provided when the contact model is interfaced with a fluid model of waves.

2.3 Order parameters

For purposes of the assessment of damage in the field, damage S is defined using the cross-sectional area A of erosion and the nominal diameter of the armour units D_n (Van der Meer, 1988) by $S = A/D_n^2$. In a numerical simulation where the positions of the armour units are available, a natural measure of damage is the root-mean-square displacement δ_{rms} of the units,

$$\boldsymbol{\delta_{rms}^2 = \frac{1}{N}\sum_{i=1}^{N}|\bar{c}_i' - \bar{c}_i|^2} \quad (3)$$

where $\bar{c}_i'$ and $\bar{c}_i$ are the final and initial displacements of unit i from the origin and N is the number of units. In an earlier paper (Greben et al., 2012), δ_{rms} is related to S.

For calculation of δ_{rms}, initial and final positions of units are required. It is useful to have an order parameter that depends only on the states of the armour units at one instant. A survey of the relevant literature showed that orientational order parameters have practical application in the fields of liquid crystals and phase changes in crystals. Molecules of an elongated shape may be aligned in a particular direction, which is defined by a vector called the director which is likely to be related to a stress vector or an electric field, or may have some degree of random alignment. The dynamics of alignment were originally explored by Onsager (Onsager, 1949) and later extended by Maier and Saupe (Maier & Saupe, 1958), and molecular dynamics simulations have been carried out for simulation of rheology with a number of shapes (Dlugoroglorski et al., 1994). From the related literature we have chosen the Vieillard-Baron order parameter (Vieillard-Baron, 1972)

$$\boldsymbol{P_2 = \frac{1}{2}\sum_{i=1}^{N}(3cos^2 w_i - 1)}\ , \quad (4)$$

where N is the number of particles and w_i is the angle between each of the molecule's long axis and the director. The parameter has the advantages of simplicity and usefulness (Gledhill et al., 2012). For these purposes we define a director vector <*Y*> as the average

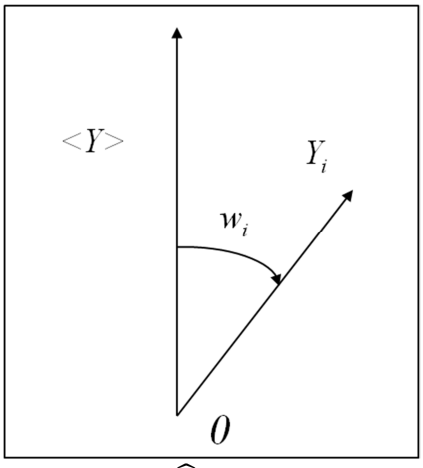

direction of the unit orientation axes, the $\widehat{Y}_\iota$, and the angle w_i as the angle between the director and the $\widehat{Y}_\iota$ (Figure 3).

Figure 3 Angle between director and orientation axis of a unit

For a random distribution of orientations $P_2 = 1/4$, while for perfect alignment, P_2 =1. When all unit axes are perpendicular to the director, $P_2 = -1/2$.

In an earlier paper (Gledhill et al., 2012), two test sample packings were used to demonstrate the expected variation of P_2. Dolosse were laid in a regular lattice on a flat horizontal slope (with no random height field). In packing test 1, uniform spacing greater than D_n was used to minimise interaction between neighbours in the first layer. Three rows were laid in each of three layers (Figure 4 a, b, c). In packing test 2, the dolosse were laid but with a denser packing (Figure 4 d, e, f). Layers are numbered from lowest to highest. Rows are numbered from front to back. The first layer consists of units laid with the same orientation, but the next two are laid with varying angles about the *y* axis, using a uniform random distribution of angles between -20º and 20º.

Dolosse were chosen for this test because of their interlocking shapes, and the expected disorder of the upper layers. The test serves to illustrate that the first layer is highly ordered ($P_2 \sim 1$ for layer 1, rows 1 to 3) and the next two layers are disordered, as shown in Figure 5.

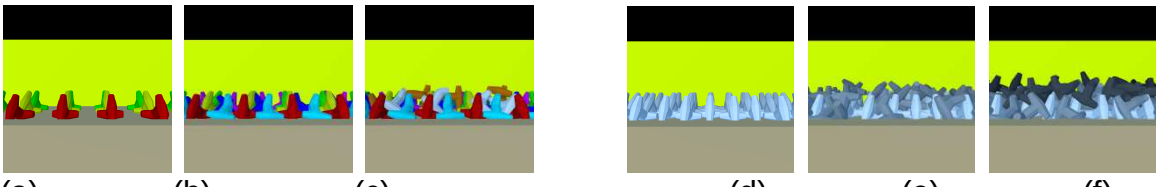

(a) (b) (c) (d) (e) (f)

Figure 4 (a), (b), (c) Sparse packing test 1; (d), (e), (f) denser packing test 2

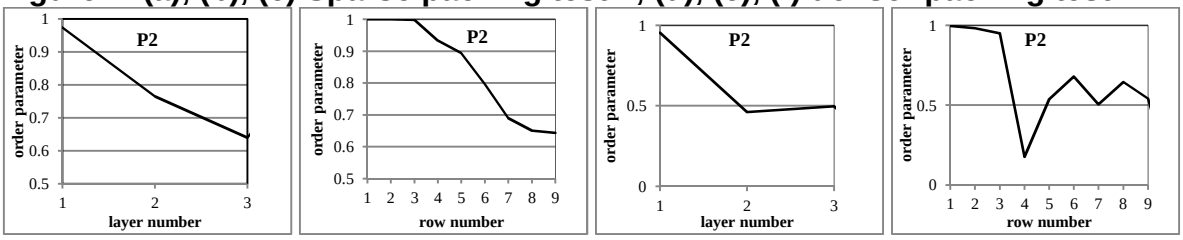

(a) (b) (c) (d)

Figure 5 Order parameter P_2 (a) sparse packing test 1, by layer; (b) sparse packing test 1, by row; (c) dense packing test 2, by layer; (d) dense packing test 2, by row

In the present paper, we proceed to compare and contrast P_2 and δ_{rms} for the same configurations, and investigate the effect of the height field and of wave perturbations.

3 Results

3.1 Statistical considerations

In complex systems of large numbers of units, where there is some degree of random variation, different initial configurations can be obtained. To test the statistical variation of δ_{rms} and P_2, we consider an ensemble (set) of initial configurations, test 3, with two important differences from test 2 above: (1) all the dolosse are in exactly the same orientation when they are lowered from a crane position, and (2) the slope has a random height field. The amplitude of the height field *h* is unvaried in each ensemble, but the random numbers used to generate the height field are changed for each simulation. Each case, therefore, has a slightly different packing. Test 3 has been run for two different values of *h*. The dolos has been chosen for this test because small variations in the random underlayer cause large variations in packing. The parameter δ_{rms} from equation (3) requires final and initial positions $\overline{c_i}'$ and $\overline{c_i}$. For the purposes of this test, the regular initial crane positions have been used, but the *y* components are neglected: only *x* and *z* are used (Figure 6).

Averages and standard deviations for 16 simulations for each value of *h* are shown in Table 1.

Table 1 Test 3 results

h	δ_{rms}	P_2
0.2 m	1.56±0.04 m	0.88±0.09
0.4 m	1.53±0.08 m	0.86±0.09

These results are plotted in the context of *h* variation below.

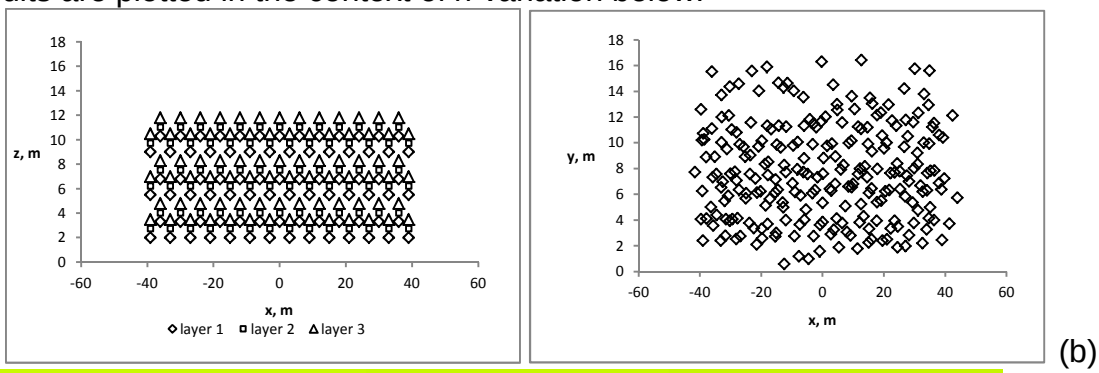

(a) (b)

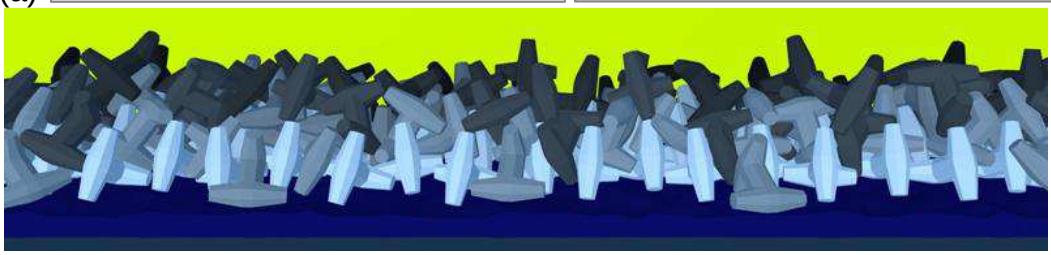

(b)

Figure 6 (a) Initial (crane) and (b) final positions (x_i, z_i) for test 3, *h* = 0.4 m (c) final positions for a sample case

3.2 Dependence of order parameters on height field

Having estimated the statistical effects for two heightfields, we proceed to consider the effect of the amplitude of the heightfield on the order parameters. Results for single cases of the test 3 configuration are shown in Figure 7. Random variation is not possible in the *h*=0 m case.

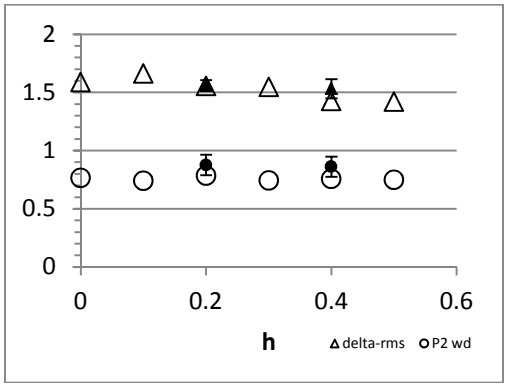

Figure 7 Dependence of order parameters on height field; filled symbols are from Table 1

It is has been shown that δ_{rms} and P_2 are providing independent information (there is a Pearson correlation coefficient of -0.01 for the data given above). With varying heightfield amplitude, δ_{rms} decreases, but the trend is close to the limits of the standard deviation calculated above; the migration of the units is approximately 1.6 m on the smooth slope and 1.4 m on the roughest slope. This suggests, in agreement with experience, that a rougher height field leads to more stability. The orientational parameter P_2 does not vary appreciably over the range of *h*. This conveys the interpretation that an underlayer with height variations of about 0.4 m does not appreciably change the orientation organisation of the assembly.

3.3 Dependence of Antifer packing randomness on wave perturbation

A simple model of an oscillating disturbance is described in section 2.2 above. If *n* waves are applied to a highly organised structure, such as an Antifer packing with two layers, it is suggested that changes in disorder could be quantified.

Antifers packed in a regular lattice are chosen for this experiment (Van der Meer & Heydra, 1991). The angle of the flat slope to the horizontal is 26.6º, and the slope is 20m high and has a horizontal crest. Walls provide boundaries in *x* and *z* and a toe is present. Low wave numbers *n* are used. For this simulation, F_0 = 15 kN, T = 8 s, k ~ 0.01 m^{-1} (approximated from the deep water dispersion relation for ocean waves). Data from a previous paper (Gledhill et al., 2012) show that a succession of n = 25 waves provides successive disordering of the packing, with P_2decreasing from 0.94 in all layers to 0.80 in the lower layer and 0.88 overall.

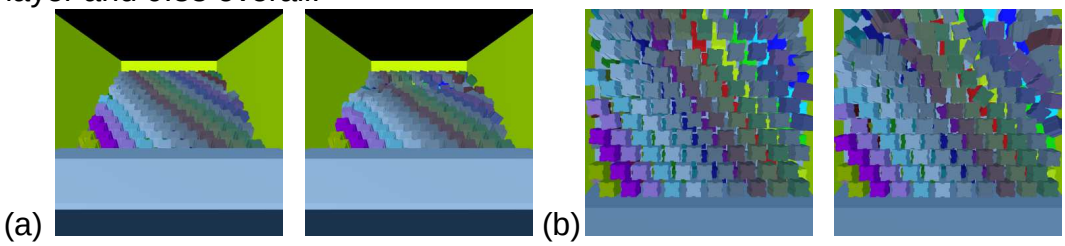

Figure 8 Antifer packing (a) before and (b) after 25 waves, from the waterline and from above

The next step is to contrast δ_{rms} and P_2 for different *n.* The results are shown in Figure 9.

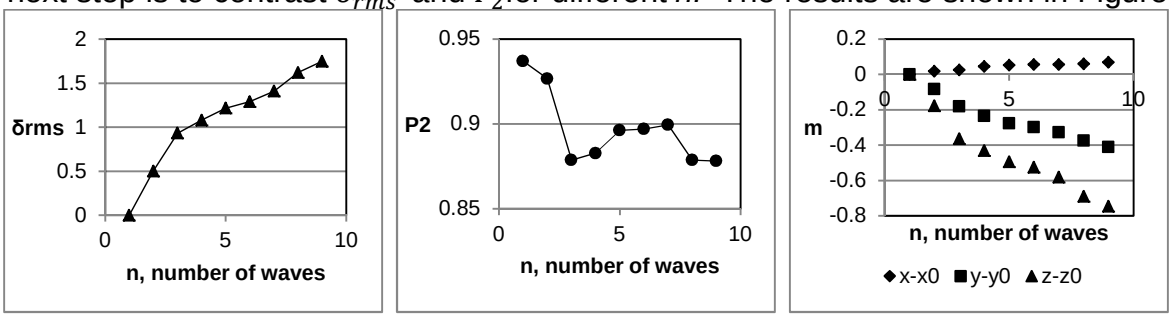

(a) (b) (c)

Figure 9 (a,b) Order parameters and (c) average displacement for waves in Antifer packing

It can again be shown that δ_{rms} and P_2 are independent. The parameter δ_{rms} increases steadily and, when compared with average displacement, is indicative of the movement down the slope that can be observed in

Figure 8 and Figure 9(c). Orientational order decreases sharply over the first few waves, and then recovers; this is likely to be due to re-ordering of units as they come into contact with one another, and is related to the same phenomena of alignment observed in other granular media when compacted by an oscillating disturbance.

4 CONCLUSIONS

This is the first time that δ_{rms} and P_2 have been compared for the same simulations. The two measures exhibit different behaviour and provide different information. The root-mean-square displacement δ_{rms} does indeed show disorder through average movement, and P_2 is a useful measure of orientational order and the alignment of units in the packing. Together, these can be used to answer the questions posed at the beginning of the paper, "How much change has taken place in armour unit position?" and "How random is the packing?" Moreover, P_2 is becoming amenable to measurement in the field with the development of more accurate photogrammetric techniques.

In future work, much remains to be done on validation with experimental and field data, and practical use.

Acknowledgements

This collaborative project was performed under the Strategic Research Panel Thematic programme of the CSIR, project TA-2008-027. The authors thank David Phelps and Dr Wim van der Molen of CSIR Coastal Engineering for their patience and their invaluable collaboration. The problem was originally posed by Dr J. van der Meer.

5 REFERENCES

Araki, S. & Deguchi, I., 2011. Numerical Simulation on Displacement of Armor Block on submerged Breakwater with 3-Dimensional DEM. In *Proc. 21st Int. Offshore and Polar Eng. Conf.* Maui, Hawaii, 2011.

Cundall, P.A. & Strack, O.D.L., 1979. A discrete numerical model for granular assemblies. *Geotechnique*, 29, pp.47-65.
Dentale, F., Carratelli, E.P., Russo, S.D. & Mascetti, S., 2009. *Advanced Numerical Simulations on the Interaction Between Waves and Rubble Mound Breakwaters*. Technical Report. University of Salerno.
Dlugoroglorski, B.D., Grmela, M., Carreau, P.J. & Lebon, G., 1994. Rheology of several hundred rigid bodies. *J. Non-Newtonian Fluid Mechanics*, 53, pp.25-64.
Frens, A.J., van Gent, M.R.A. & Olthof, J., 2008. Placement methods for antifer armour units. Hamburg, 31 Aug- 5 Sept 2008.
Gledhill, I.M.A., Greben, J.M., de Villiers, R. & Cooper, A.K.a.G.J.-H., 2012. The use of orientational order parameters for characterisation of coastal breakwaters. In *8th SA Conf. on Computational and Applied Mechanics SACAM*. Johannesburg, 2012. SAAM.
Govender, K., Alport, M.J. & Mocke, G.a.M.H., 2002. Video measurements of fluid velocities and water levels in breaking waves. *Physica Scripta*, T97, pp.152-59.
Greben, J.M. Gledhill, I.M.A., Cooper, A.K., De Villiers, R. & Van der Meer, J.M., 2012. Damage to breakwaters simulated by a physics engine. *in preparation*.
Grobler, J.H., De Villiers, R. & Cooper, A.K., 2010. Modelling of fluid-solid interaction though two stand-alone codes. In *7th South African Conference on Computational and Applied Mechanics, SACAM10*. Pretoria, 2010.
Hahn, J.K., 1988. Realistic animation of rigid bodies. In *Proc. 15th Annual Conference on Computer Graphics and Interactive Techniques SIGGRAPH '88*., 1988. ACM.
Latham, J.-P. et al., 2008. Three-dimensional particle shape acquisition and use of shape library for DEM and FEM/DEM simulation. *Minerals Engineering*, 21, pp.797-805.
Latham, J.-P., Munjiza, A. & Lu, Y., 2002. On the prediction of void porosity and packing of rock particulates. *Powder Technology*, 125, pp.10-27.
Latham, J.P. et al., 2008. Modelling of massive particulates for breakwater engineering using coupled FEMDEM and CFD. *Particuology*, 6, pp.572-83.
Maier, W. & Saupe, A., 1958. Ein einfache molekulare Theorie des nematischen kritallenflussiger Zustandes. *Z. Naturforschung*, 18, pp.379-89.
Mukaro, R., Govender, K., Gledhill, I. & Kokwe, N.L., 2010. Velocity flow field and water level measurements in shoaling and breaking water waves. In *7th SA Conf. on Computational and Applied Mechanics, SACAM10*. Pretoria, 2010.
Müller, M., Stam, J., James, D. & Thürey, N., 2008. Real Time Physics. In *Annual Conference on Computer Graphics and Interactive Techniques SIGGRAPH '08*., 2008.
Munjiza, A., 2004. *The Combined Finite-Discrete Element Method*. Wiley.
Munjiza, A., 2011. *Computational mechanics of discontinua*. John Wiley and Sons.
NVIDIA, 2012. *PhysX*. [Online] Available at: HYPERLINK "file:///D:\\igle%20projects\\2012\\2012Ports\\satc2013\\www.nvidia.com" www.nvidia.com [Accessed March 2012].
Onsager, L., 1949. The effects of shape on the interaction of colloidal particles. *Annals of the New York Academy of Sciences*, pp.627-59.
Owen, D.R.J. et al., 2004. The modelling of multi-fracturing solids and particulate media. *Int. J. Num. Methods in Engineering*, 60, pp.317-39.
Van der Meer, J., 1988. *Rock slopes and gravel beaches under wave attack.* Delft: Technical University of Delft, Ph.D. Thesis.
van der Meer, J.W., 1995. Conceptual design of rubble mound breakwaters. In Liu, P.L.F. *Advances in Coastal and Ocean Engineering Vol. 1*. World Scientific. pp.221-315.
Van der Meer, J. & Heydra, G., 1991. Rocking armour units: Number, location and impact velocity. *J. Coastal Engineering*, 15, pp.21-39.
Vieillard-Baron, J., 1972. Phase transitions of the hard-ellispe system. *J. Phys. Chem.*, 56, p.4729.

Vieira, R., van den Bergh, F. & van Wyk, B.J., 2008. Fiducial-based monocular 3D displacement measurement of breakwater armour unit models. In *19th Annual Symposium of the Pattern Recognition Association of South Africa (PRASA 2008)*., 2008.
Xiang, J., Munjiza, A., Latham, J.-P. & and Guises, R., 2010. On the validation of DEM and FEM/DEM models in 2D and 3D. *Engineering Computations*, 26(6), pp.673-87.